

Saturation from nuclear pion dynamics

M. Lutz^a, B. Friman^{a,b} and Ch. Appel^a

^a *GSI, Planckstr. 1, D-64291 Darmstadt, Germany*

^b *Institut für Kernphysik, TU Darmstadt, D-64289 Darmstadt, Germany*

Abstract

We construct an equation-of-state for nuclear matter based on the chiral Lagrangian. The relevant scales are discussed and an effective chiral power expansion scheme, which is constructed to work around the nuclear saturation density, is presented. A realistic equation-of-state is obtained by adjusting *one* free parameter, when the leading and subleading terms in the expansion are included. The saturation mechanism is due to correlations induced by the one-pion-exchange interaction. Furthermore, we find a substantial deviation from the Fermi-gas estimate of the quark condensate in nuclear matter already at the saturation density.

For more than four decades, one of the basic problems of nuclear physics has been to find a microscopic understanding of the nuclear equation-of-state in terms of the free nucleon-nucleon interaction [1–3]. The present status is that a quantitative description of nuclear matter can be achieved in a non-relativistic approach only by invoking a three-body force [5], or alternatively with the lowest-order term in the relativistic Brueckner approach [4]. A drawback of the latter, is the lack of a systematic expansion scheme. Thus, it has so far not been possible to obtain a reliable estimate for the corrections to the leading term. Such calculations are based on the traditional semi-phenomenological approach to the nucleon-nucleon interaction, represented by e.g. the Urbana-Argonne [6] and Bonn [7] potentials.

During the last few years, a novel approach to the nucleon-nucleon interaction, based on chiral perturbation theory (χ PT), has started to emerge. A key element in χ PT is the power counting, which relies on a separation of scales. This allows one to organize a systematic approximation scheme. In the nuclear many-body problem, new scales enter, which requires a modification of the expansion scheme developed for the nucleon-nucleon interaction in free space. In this letter we identify the new scales and present an effective chiral perturbation theory, appropriate for the nuclear many-body problem. We employ this scheme to construct a nuclear equation-of-state and compute the quark condensate in nuclear matter.

The key element of any microscopic theory for the nuclear equation-of-state is the elementary nucleon-nucleon interaction. In the context of chiral perturbation theory this problem was first addressed by Weinberg who proposed to derive a chiral nucleon-nucleon potential in time ordered perturbation theory [8,9]. An alternative scheme, with chiral power counting rules applied directly to the nucleon-nucleon scattering amplitude, was subsequently proposed [10–12]. This approach relies on the crucial observation that the chiral power counting rules can be generalized for 2-nucleon reducible diagrams. Non-perturbative effects like the pseudo bound state pole in the 1S_0 channel are generated by properly renormalized local two-nucleon vertices, that carry an anomalous chiral power Q^{-1} .

The counting rules for the vacuum nucleon-nucleon scattering amplitude provide a suitable starting point for the construction of chiral power counting rules for the nuclear matter problem [13]. The density expansion, or equivalently the multiple scattering expansion, is readily combined with the chiral expansion, once one identifies the Fermi momentum $k_F \sim Q$ as a further small scale. This identification leads to a systematic partial resummation of the density expansion, where one avoids the expansion in large ratios like k_F/m_π but exploits the chiral mass gap and expands in small ratios like k_F/m_χ and m_π/m_χ with $m_\chi \simeq 4\pi f_\pi \simeq 1$ GeV.

In the generalized chiral power expansion scheme [10–12], the nucleon-nucleon scattering amplitude is expanded in the small ratio Q/Λ_L , but not in the large one Q/Λ_S , where $\Lambda_L \simeq m_\chi$ and Λ_S is a small scale, like $\sqrt{m_N \epsilon_D}$ where $\epsilon_D \simeq 2$ MeV is the binding energy of the deuteron. This leads to an expansion of the scattering amplitude of the generic form

$$\mathcal{M}(Q) = \sum_n \mathcal{M}_n \left[\frac{Q}{\Lambda_S} \right] \left(\frac{Q}{\Lambda_L} \right)^n, \quad (1)$$

where the small scale Q is identified with the nucleon momentum or the mass of the pion m_π . An immediate consequence of the chiral expansion schemes, is that the long-range part of the one-pion-exchange interaction can be treated perturbatively. The short-ranged or large-momentum part is, as described below, effectively included in the local part of the chiral Lagrangian, which is treated non-perturbatively.

When this scheme is applied to the nuclear many-body problem one finds that the pion dynamics remains perturbative in the sense discussed above, but the local two-nucleon interaction requires extensive resummations. This is an immediate consequence of the chiral power given to the renormalized two-nucleon coupling $g_R \sim Q^{-1}$. Thus, in nuclear matter at small density, say $\rho \simeq 0.01$ fm $^{-3}$, it is not sufficient to sum only the particle-particle ladder diagrams of the local two-nucleon interaction, as is done in lowest-order Brueckner calcu-

lations. We find that one must sum also the particle-hole and hole-hole ladder diagrams including all interference terms with self-consistently dressed nucleon propagators. According to the generalized counting rules the pions can then be evaluated perturbatively on top of the parquet resummation for the local two-nucleon interaction, described above¹. In terms of vacuum scales this leads to an expansion of the energy per particle, $E(k_F)$, of the form

$$E(k_F) = \sum_n E_n \left[\frac{k_F}{m_\pi}, \frac{k_F}{\Lambda_S} \right] \left(\frac{k_F}{\Lambda_L} \right)^n. \quad (2)$$

The expansion coefficients E_n are complicated, presently unknown, functions of the Fermi momentum k_F . However, by employing appropriate resummations, these functions can be computed from the free-space chiral Lagrangian [14].

Since the typical small scale $\Lambda_S \simeq 50$ MeV is much smaller than the Fermi momentum at the saturation density, $k_F^{(0)} \simeq 265$ MeV, one may expand the coefficients E_n around $k_F^{(0)}$ in the following manner

$$E_n \left[\frac{k_F}{m_\pi}, \frac{k_F}{\Lambda_S} \right] = E_n \left[\frac{k_F}{m_\pi}, \frac{k_F^{(0)}}{\Lambda_S} \right] + \sum_{k=1}^{\infty} \bar{E}_n^{(k)} \left[\frac{k_F}{m_\pi}, \frac{k_F^{(0)}}{\Lambda_S} \right] \left(\frac{\Lambda_S}{k_F} - \frac{\Lambda_S}{k_F^{(0)}} \right)^k. \quad (3)$$

Note that we do not expand in the ratio m_π/k_F . Clearly this scheme is constructed to work around nuclear saturation density but will fail at very small densities. However, also other approaches, like the Walecka model [17] and the Brueckner scheme, are not reliable at very low densities.

Physically the expansion (3) may be interpreted in the following way. The parquet resummation of the local nucleon-nucleon interaction gives rise to a density dependence governed by the scale Λ_S , while the relevant scale for the pion dynamics is m_π . If $\Lambda_S/k_F^{(0)}$ is so small, that the parquet resummation is close to its high-density limit at normal nuclear matter density, the expansion (3) converges rapidly, and we can, as a first approximation, retain only the leading term in this expansion. In this case the density dependence of the coefficients of the expansion (2) is, to a very good approximation, given by the pion dynamics.

A systematic derivation of the expansion (2) and (3), applying suitable resummation techniques, will be presented elsewhere [14]. In this work we pursue a

¹ The expectation that the nuclear equation-of-state can be computed microscopically by summing the parquet diagrams for the local interaction and then including pions perturbatively may be too optimistic. A refined formulation, which incorporates the relevant subthreshold singularities of the vacuum nucleon-nucleon scattering amplitude (see [11]), may require a more involved treatment of pionic effects.

less microscopic approach. We assume that the coefficients $E_n(k_F/m_\pi, k_F^{(0)}/\Lambda_S)$ can be computed in an effective theory whose unknown parameters are adjusted to the saturation properties of nuclear matter. We employ an effective Lagrangian density, where the nucleons interact through s-wave contact interactions and through the exchange of pions. Here we do not include local p-wave nor three-body interaction terms since they do not contribute to leading and subleading order in the chiral expansion. The interaction part of the Lagrangian is given by

$$\begin{aligned}\mathcal{L}_{int}(k_F) = & \frac{g_A}{2f_\pi} N^\dagger (\sigma \cdot \nabla) (\pi \cdot \tau) N \\ & + \frac{1}{8f_\pi^2} \left(g_0(k_F) + \frac{1}{4} g_A^2 \right) (N^\dagger N)_1 P_{12}^{S=1, T=0} (N^\dagger N)_2 \\ & + \frac{1}{8f_\pi^2} \left(g_1(k_F) + \frac{1}{4} g_A^2 \right) (N^\dagger N)_1 P_{12}^{S=0, T=1} (N^\dagger N)_2\end{aligned}\quad (4)$$

where N is the two component nucleon spinor field and P_{12}^{ST} is the projection operator for a two-nucleon state with spin S and isospin T . Note that in the contact interaction the spatial coordinates of the two particles are identical. The terms proportional to $g_A^2/4$ are counter terms, which cancel the local, high momentum, piece of the one-pion-exchange interaction. Below we discuss the role of the counter terms in more detail.

Rather than evaluating the coefficients of the chiral density expansion (2,3), we compute the energy directly. The coefficients E_n can be extracted from the resulting expressions. In Fig. 1 we show all diagrams of chiral order Q^3 and Q^4 . They correspond to the leading and subleading interaction contributions to (2). The dashed line is the pion propagator. We split the non-interacting nucleon propagator into a free-space part

$$S_N(p_0, \mathbf{p}) = \frac{1}{p_0 - \mathbf{p}^2/(2m_N) + i\epsilon}, \quad (5)$$

denoted by a directed solid line, and a density-dependent part

$$\Delta S_N(p_0, \mathbf{p}) = 2\pi i \delta(p_0 - \mathbf{p}^2/(2m_N)) \Theta(k_F^2 - \mathbf{p}^2) \quad (6)$$

represented by a line with a 'cross'. Thus, depending on the diagram, such a line corresponds to a hole line or the Pauli blocking of a particle line. This separation is useful for the expansion scheme we adopt.

The pion dynamics which is computed explicitly in our scheme. If properly renormalized, it is perturbative like in the vacuum case. The non-perturbative short-range physics is subsumed in the local interaction. In our scheme, the

power counting is much simpler than in a fully microscopic one, where one would have to sum diagrams involving the small scales Λ_S and k_F to all orders. This infinite set of diagrams is already included in our interaction constants $g_0(k_F)$ and $g_1(k_F)$. Consequently, in order to avoid double counting, diagrams with two or more adjacent interaction vertices g_0 or g_1 are forbidden. Therefore we introduce two types of local 2-nucleon vertices in Fig. 1. The filled circle represents the full zero-range vertex of (4) proportional to $g_{0,1} + g_A^2/4$ while the open circle corresponds to only the counter term proportional to $g_A^2/4$. Clearly there are no diagrams of the type e-f in Fig. 1 with the full contact interaction (filled circles) at both vertices.

Note, that in our counting g_0 and g_1 are of order Q^0 since the non-perturbative structures like the deuteron, which give rise to the anomalously large amplitude $\sim Q^{-1}$ in vacuum, are dissolved at densities far below the saturation density. We neglect the density dependence of the effective coupling constants g_0 and g_1 . This corresponds to retaining only the leading term in (3). We can test whether subleading terms are required, by allowing the coupling constants to be density dependent.

The contribution of the first diagram in Fig. 1 to the ground state energy density ϵ is proportional to $(g_0(k_F) + g_1(k_F)) k_F^6$. Since the effective vertices $g_0(k_F), g_1(k_F) \sim Q^0$ carry chiral power zero, this diagram is of chiral order Q^6 . The contribution to the energy per particle $E(k_F) = \epsilon(k_F)/\rho$ is of order Q^3 , since $\rho = 2k_F^3/(3\pi^2)$. In this paper, the chiral power of a diagram is defined by its contribution to the energy per particle. The one pion exchange contribution (Fig. 1 b), is also of chiral order Q^3 since it is proportional to k_F^3 times a dimension less function of k_F/m_π .

The leading interaction contributions to the energy per particle (Fig. 1 a,b) can be expressed in terms of a momentum dependent effective scattering amplitude $T_{eff}(p)$:

$$E_T(k_F) = -\frac{k_F^3}{2\pi^2} \int_0^1 x^2 dx (1-x)^2 (2+x) T_{eff}(k_F x) \quad (7)$$

where

$$T_{eff}(p) = \frac{3}{f_\pi^2} \left(g_0 + g_1 + \frac{g_A^2}{2} \right) - \frac{3}{2} \frac{g_A^2}{f_\pi^2} \frac{4p^2}{m_\pi^2 + 4p^2}. \quad (8)$$

In (8) the cancellation between the counter terms in the local effective interaction (4) and the high-momentum part from the one-pion-exchange interaction is evident. As an example for the link between the Lagrangian (4) and the chiral density expansion, we consider the coefficient $E_3[k_F/m_\pi, k_F^{(0)}/\Lambda_S]$

in (3). The contribution of the contact interaction is given by $E_3/\Lambda_L^3 = -2(g_0 + g_1)/(4\pi f_\pi)^2$. We note that the small scale Λ_S is hidden in the coupling constants g_0 and g_1 .

Next we consider the diagrams of subleading order, shown in Fig. 1. These diagrams fall into two distinct classes: those with two and three crosses. We do not show the diagrams with four crosses since their real parts vanish and their imaginary parts cancel that of the other diagrams so that, to a given order, the resulting energy is real. Furthermore, we do not include vacuum-polarization diagrams and vacuum vertex renormalization diagrams. The former vanish in a non-relativistic scheme², while the latter are suppressed by two chiral powers Q^2 .

We note that after a proper renormalization, diagrams with only one cross are implicitly included in the kinetic energy term

$$E_{\text{kin}}(k_F) = \frac{3}{10} \frac{k_F^2}{m_N}. \quad (9)$$

The contribution of diagrams d), f), h), j) and l) with two crosses can again be expressed in terms of an effective scattering amplitude $T_{eff}(p)$ with

$$\begin{aligned} T_{eff}^{(d+f)}(p) &= 6 \frac{g_A^2}{f_\pi^4} \left(g_0 + g_1 + \frac{g_A^2}{4} \right) m_N^2 I(p) \\ T_{eff}^{(h)}(p) &= 3 \left(g_0 + g_1 + \frac{g_A^2}{2} \right) \frac{g_A^2}{2 f_\pi^4} \frac{m_N m_\pi^2}{8 \pi p} i \log \left(1 - 2i \frac{p}{m_\pi} \right) \\ &\quad - 6 \left(g_0 + g_1 + \frac{g_A^2}{2} \right) \frac{g_A^2}{f_\pi^4} m_N^2 I(p) \\ T_{eff}^{(j)}(p) &= \frac{3 g_A^4}{4 f_\pi^4} \frac{m_N m_\pi^2}{4 \pi} \left(\frac{1}{m_\pi - 2i p} - 2 \frac{i}{p} \log \left(1 - 2i \frac{p}{m_\pi} \right) \right) \\ &\quad + 6 \frac{g_A^4}{f_\pi^4} m_N^2 I(p) \\ T_{eff}^{(l)}(p) &= \frac{3 g_A^4}{2 f_\pi^4} \frac{m_N m_\pi^2}{4 \pi} \left(\frac{m_\pi^4 + 8 m_\pi^2 p^2 + 8 p^4}{16 p m_\pi^3 (m_\pi^2 + 2 p^2)} \left(i \log \left(1 + 4 \frac{p^2}{m_\pi^2} \right) \right. \right. \\ &\quad \left. \left. + \arctan \left(\frac{p}{m_\pi} \left(3 + 4 \frac{p^2}{m_\pi^2} \right) \right) - \arctan \left(\frac{p}{m_\pi} \right) \right) \right. \\ &\quad \left. - \frac{i p}{2 m_\pi^2} \log \left(1 - 2i \frac{p}{m_\pi} \right) \right) - \frac{3 g_A^4}{2 f_\pi^4} m_N^2 (I(p) - 2 I(i m_\pi)). \quad (10) \end{aligned}$$

² The non-relativistic scheme presented here is identical with the non-relativistic reduction of a relativistic scheme order by order in the chiral expansion [11].

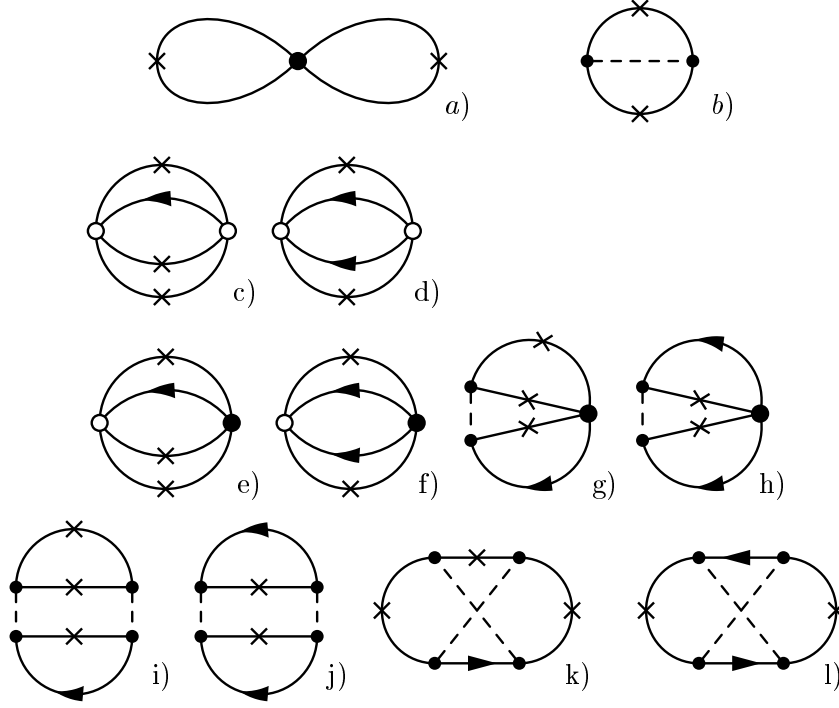


Fig. 1. Leading and subleading contributions to the energy of nuclear matter. The Feynman rules are explained in the text.

The loop integral $I(p)$ is divergent and must be regularized:

$$I(p) = \frac{1}{8\pi^2 m_N} \int_0^\Lambda \frac{l^2 dl}{l^2 - p^2 - i\epsilon} = \frac{1}{16\pi m_N} \left(\frac{2}{\pi} \Lambda + ip + \mathcal{O}\left(\frac{p^2}{\Lambda^2}\right) \right). \quad (11)$$

Here Λ is a cutoff parameter.

In (10) the appropriate symmetry factors are included. We note that the diagrams d), f), h), j) and l) in Fig. 1 are all divergent. However, the sum of all diagrams is finite once we include a further counter term in the spin triplet channel:

$$g_0 \rightarrow g_0 - \frac{m_N \Lambda}{4\pi^2} \frac{g_A^4}{f_\pi^2}. \quad (12)$$

This counter term, which is formally of order Q , cancels the divergence due to the second-order tensor interaction. Collecting all real terms from (8) and (10) we find

$$T_{eff}(p) = \frac{3}{f_\pi^2} (g_0 + g_1) + \frac{3}{2} \frac{g_A^2}{f_\pi^2} \frac{m_\pi^2}{m_\pi^2 + 4p^2}$$

$$\begin{aligned}
& + \frac{3 g_A^2}{f_\pi^2} (g_0 + g_1) \frac{m_\pi m_N}{16\pi f_\pi^2} \frac{m_\pi}{p} \arctan\left(\frac{2p}{m_\pi}\right) \\
& + \frac{3 g_A^4}{f_\pi^2} \frac{m_\pi m_N}{16\pi f_\pi^2} \left(\frac{m_\pi^2}{m_\pi^2 + 4p^2} - \frac{3}{2} \frac{m_\pi}{p} \arctan\left(\frac{2p}{m_\pi}\right) \right) \\
& + \frac{3 g_A^4}{f_\pi^2} \frac{m_\pi m_N}{16\pi f_\pi^2} \left(-\frac{p}{m_\pi} \arctan\left(\frac{2p}{m_\pi}\right) - 1 \right. \\
& + \frac{m_\pi^4 + 8 m_\pi^2 p^2 + 8 p^4}{8 p m_\pi (m_\pi^2 + 2 p^2)} \left(\arctan\left(\frac{p}{m_\pi} \left(3 + 4 \frac{p^2}{m_\pi^2}\right)\right) \right. \\
& \left. \left. - \arctan\left(\frac{p}{m_\pi}\right) \right) \right) \Bigg). \tag{13}
\end{aligned}$$

The corresponding contribution to the energy per particle is again given by Eq. (7).

We now turn to the remaining diagrams c), e), g), i) and k). Their contribution to the energy per particle reads

$$\begin{aligned}
E_P(k_F) = & \frac{m_N k_F^4}{(4\pi f_\pi)^4} \left(\frac{3}{2} g_A^2 \left(g_0 + g_1 + \frac{g_A^2}{4} \right) J_0 \right. \\
& \left. - \frac{3}{2} g_A^2 \left(g_0 + g_1 + \frac{g_A^2}{2} \right) J_1(k_F) + \frac{3}{2} g_A^4 J_2(k_F) - \frac{3}{8} g_A^4 J_3(k_F) \right) \tag{14}
\end{aligned}$$

where

$$\begin{aligned}
J_{n<3}(k_F) = & \frac{24}{k_F^7} \int_0^{k_F} \mathbf{q}^2 d\mathbf{q} \int_{-1}^1 dx_{\mathbf{q}} \left(k_F |\mathbf{q}| x_{\mathbf{q}} + \frac{k_F^2 - \mathbf{q}^2 x_{\mathbf{q}}^2}{2} \log \frac{k_F + |\mathbf{q}| x_{\mathbf{q}}}{k_F - |\mathbf{q}| x_{\mathbf{q}}} \right) \\
& \cdot (F_n(0) - F_n(\lambda(\mathbf{q}, x_{\mathbf{q}}))) \\
J_3(k_F) = & \frac{24}{k_F^7} \int_0^{k_F} \mathbf{p}^2 d\mathbf{p} \int_{-1}^1 x_{\mathbf{p}} dx_{\mathbf{p}} \int_{-1}^1 x_{\mathbf{q}} dx_{\mathbf{q}} \left(\frac{\Theta(x_{\mathbf{q}}^2 + x_{\mathbf{p}}^2 - 1)}{\sqrt{x_{\mathbf{q}}^2 x_{\mathbf{p}}^2 (x_{\mathbf{q}}^2 + x_{\mathbf{p}}^2 - 1)}} - 2 \right) \\
& \cdot (F_1(\lambda(\mathbf{p}, x_{\mathbf{q}})) - F_1(0)) (F_1(\lambda(\mathbf{p}, x_{\mathbf{p}})) - F_1(0)) \tag{15}
\end{aligned}$$

and

$$\begin{aligned}
\lambda(\mathbf{q}, x_{\mathbf{q}}) = & \sqrt{k_F^2 - \mathbf{q}^2(1 - x_{\mathbf{q}}^2)} - |\mathbf{q}| x_{\mathbf{q}} \\
F_0(l) = & \frac{l^2}{2} \\
F_1(l) = & \frac{l^2}{2} - \frac{m_\pi^2}{2} \log(l^2 + m_\pi^2)
\end{aligned}$$

$$F_2(l) = \frac{l^2}{2} - \frac{m_\pi^4}{2(l^2 + m_\pi^2)} - m_\pi^2 \log(l^2 + m_\pi^2). \quad (16)$$

The integral J_0 can be performed analytically with the result $J_0 = 16(11 - \ln 4)/35$.

The resulting equation-of-state is given by $E(k_F) = E_{kin} + E_T + E_P$. We note that in symmetric nuclear matter there is effectively only one free parameter, namely the effective coupling constant $g = g_0 + g_1$, since we neglect the density dependence of g_0 and g_1 , as discussed above. In Fig. 2 we show the energy per nucleon for $g = 2.8, 3.0, 3.2, 3.4$ and 3.6 . We emphasize that the coupling functions $g_0(k_F), g_1(k_F)$ are to be determined from the nuclear equation-of-state. Thus, by allowing $g_0(k_F)$ and $g_1(k_F)$ to be arbitrary functions of k_F we could have trivially obtained a realistic equation-of-state. However there is a strong consistency constraint: according to our scale argument discussed above, the density dependence of the coupling functions must be weak for k_F larger than the small scales, which formally have been integrated out. Thus, our scheme would have to be rejected, had we found a strong density dependence of g_0 and g_1 . In fact, the density independent set of parameters $g \simeq 3.23$, $g_A \simeq 1.26$, $m_\pi \simeq 140$ MeV and $f_\pi \simeq 93$ MeV yields an excellent equation-of-state. We obtain saturation at the Fermi momentum $k_F^{(0)} \simeq 265$ MeV, which corresponds to a density $\rho_0 \simeq 0.16 \text{ fm}^{-3}$, in agreement with the empirical value. Furthermore, the empirical binding energy of 16 MeV is reproduced and we obtain an incompressibility of $\kappa \simeq 218$ MeV, compatible with the empirical value (210 ± 30) MeV of ref. [16].

It is interesting to explore the convergence properties of the expansion (2). At the saturation density, the leading term of chiral order Q^2 (the kinetic energy) contributes 22.5 MeV to the energy per particle $E(k_F)$, the terms of order Q^3 (Fig. 1 a-b) contribute -93.5 MeV and the terms of order Q^4 (Fig. 1 c-l) $+55.0$ MeV. We observe a partial cancellation between the Q^3 and Q^4 terms. However, based on these terms alone, one can draw only qualitative conclusions on the convergence properties of the expansion. Quantitative results have to await the evaluation of terms of higher order in Q . As one finds e.g. for the hole-line expansion in Brueckner theory [2], it may well be that the convergence is in fact much better than suggested by the first few (fairly large) terms.

The saturation mechanism of our model is quite different from that of popular effective models, like the Skyrme and Walecka models. In the Skyrme model the saturation is due to the density and velocity dependence of the zero-range effective interaction [16], while in the Walecka model it is a relativistic effect [17]. In neither of these models are pionic degrees of freedom explicitly included. In our model, on the other hand, saturation is obviously due to pion dynamics, since for $g_A = 0$ only the diagram in Fig. 1a survives and g_0 and g_1 are independent of density. This is reminiscent of the saturation mechanism

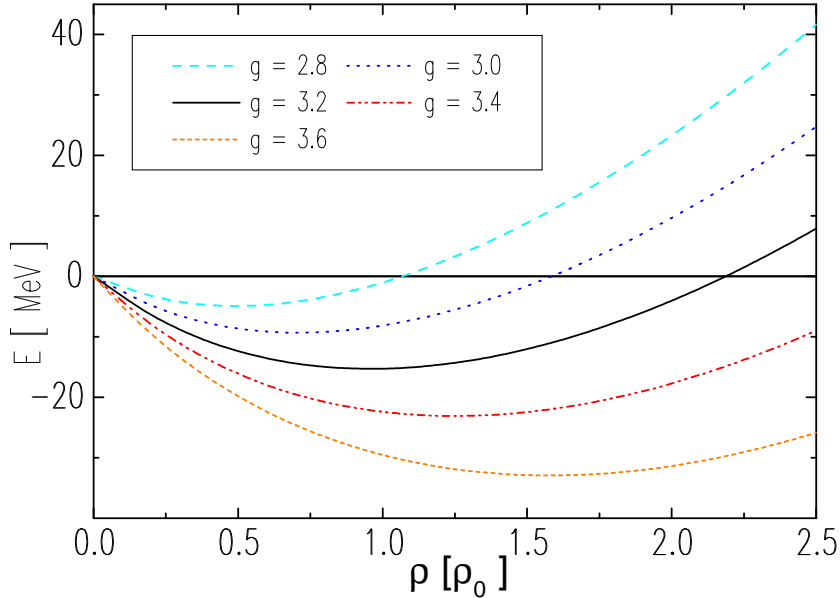


Fig. 2. The equation-of-state for isospin-symmetric nuclear matter.

in the Brueckner approach, which, to a large extent, is due to the second-order tensor contribution [1]. We note however that there is no one-to-one correspondence between the pion-exchange diagrams in the two approaches. For instance, the short-range part of the iterated one-pion-exchange is in our approach, through the renormalization procedure, subsumed in the zero-range interaction. Since the coupling constants g_0 and g_1 are adjusted to reproduce the properties of nuclear matter, this part of the one-pion-exchange interaction is effectively treated non-perturbatively. In the Brueckner approach, on the other hand, the divergencies are regularized by form factors. Consequently, there the corresponding finite contributions to the energy are associated with the original pion-exchange diagrams. Since the one-pion-exchange is perturbative only once the short-range part has been removed, it must be iterated to all orders in the Brueckner approach.

Our equation-of-state is useful for applications, where the pion dynamics plays an important role. As an example, we consider the quark condensate in nuclear matter. The quark condensate, $\langle \bar{q}q \rangle$, is an order parameter for the spontaneously broken chiral symmetry. Thus, its dependence on baryon density, indicates to what extent chiral symmetry is restored in nuclear matter. Furthermore, it is an important ingredient in the QCD sum rules [18] and in the Brown-Rho scaling approach [19]. According to the Feynman-Hellman theorem the quark condensate can be extracted unambiguously from the total energy per particle, $m_N + E(\rho)$, of nuclear matter, once its dependence on the current quark mass is known:

$$\langle \bar{q}q \rangle(\rho) - \langle \bar{q}q \rangle(0) = \rho \frac{\partial}{\partial m_Q} (m_N + E(\rho, m_Q)) . \quad (17)$$

Here $m_Q = (m_u + m_d)/2$ is the average of the u and d quark masses. In our approach the contribution of the pion degrees of freedom to the energy is included in a chirally consistent manner to order Q^4 . This allows us to estimate the effect of correlations on the quark condensate in nuclear matter to leading and subleading order.

It is convenient to consider the relative change of the quark condensate

$$\frac{\langle \bar{q}q \rangle(\rho)}{\langle \bar{q}q \rangle(0)} = 1 - \frac{\Sigma_{\pi N} \rho}{m_\pi^2 f_\pi^2} - \frac{\alpha_\pi(\rho) \rho}{2 m_\pi f_\pi^2} . \quad (18)$$

The penultimate term in (18) is the modification of the quark condensate in a free Fermi gas of nucleons, where

$$\Sigma_{\pi N} = m_Q \langle N | \bar{q}q | N \rangle = m_Q \frac{d m_N}{d m_Q} \quad (19)$$

is the pion-nucleon sigma term. Finally, the last term in (18) is due to the dependence of the interaction energy on the pion mass

$$\alpha_\pi(\rho) = -\frac{2 m_\pi f_\pi^2}{\langle \bar{q}q \rangle(0)} \frac{\partial}{\partial m_Q} E(\rho, m_Q) = \left(1 + \mathcal{O}(m_\pi^2)\right) \frac{\partial}{\partial m_\pi} E(\rho, m_\pi) \quad (20)$$

where we use the Gell-Mann–Oakes–Renner relation to convert the dependence on the current quark mass m_Q to a dependence on the pion mass. We emphasize that the second term on the right-hand side of (18), which was first written down in refs. [20–22], does not probe the interactions in nuclear matter. Therefore the linear density dependence of the quark condensate, which results when only this term is retained, should be considered with caution. It is a priori not clear that this term is the most important one at the saturation density and beyond.

Note that here we neglect any implicit m_π dependence of the effective couplings g_0 and g_1 , since naive counting arguments suggest that the corresponding contribution to the energy per particle would be of order Q^5 . In Fig. 3 we show the resulting quark condensate in nuclear matter. We confront the ‘leading’ term, which is proportional to the sigma term $\Sigma_{\pi N} \simeq 45$ MeV, with the full result given by (18). The inclusion of pionic interaction effects counteracts the reduction of the condensate due to the leading term. Our results confirm calculations performed within the Brueckner [23] and Dirac-Brueckner [24] approach qualitatively insofar that the nuclear many-body system reacts against

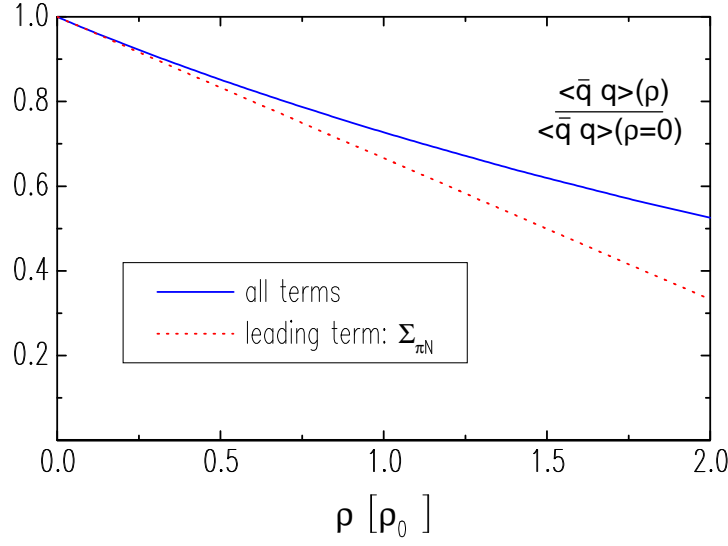


Fig. 3. The quark condensate in isospin symmetric nuclear matter.

chiral symmetry restoration. This result has important implications for the restoration of chiral symmetry in matter at finite baryon density.

References

- [1] H.A. Bethe, Ann. Rev. Nucl. Sci. **21** (1971) 93.
- [2] B.D. Day, Rev. Mod. Phys. **39** (1967) 719; Rev. Mod. Phys. **50** (1978) 495.
- [3] V.R. Pandharipande and R.B. Wiringa, Rev. Mod. Phys. **51** (1979) 821.
- [4] R. Brockmann and R. Machleidt, Phys. Rev. **C42** (1990) 1965
- [5] V.R. Pandharipande, A. Akmal and D.G. Ravenhall, in Proceedings of the International Workshop XXVI on Gross Properties of Nuclei and Nuclear Excitations, Hirschegg, Austria, 1998, pg 11.
- [6] I.E. Lagaris and V.R. Pandharipande, Nucl. Phys. **A359** (1981) 331; R.B. Wiringa, R.A. Smith and T.L. Ainsworth, Phys. Rev. **C29** (1984) 1207.
- [7] R. Machleidt, K. Holinde and Ch. Elster, Phys. Rep. **149** (1987) 1.
- [8] S. Weinberg, Phys. Lett. **B 251**(1990) 288; Nucl. Phys. **B 363** (1991) 3.
- [9] C. Ordonez, L. Ray and U. van Kolck, Phys. Rev. Lett. **13** (1994) 1982.
- [10] M. Lutz, in: *The standard Model at Low Energies*, hep-ph/9606301.
- [11] M. Lutz, nucl-th/9906028.

- [12] D.B. Kaplan, M.J. Savage and M.B. Wise, Nucl. Phys. **B 534** (1998) 329.
- [13] M. Lutz, Nucl. Phys. **A 642** (1998) 171c.
- [14] M. Lutz, in preparation.
- [15] M. Beiner et al, Nucl. Phys. **A 238** (1975) 29.
- [16] J.P. Blaizot, Phys. Rep. **64** (1980) 172.
- [17] B.D. Serot and J.D. Walecka, Adv. Nucl. Phys. **16** (1986) 1.
- [18] T. Hatsuda and Su H. Lee, Phys. Rev. **C 46** (1992) R 34.
- [19] G.E. Brown and M. Rho, Phys. Rev. Lett. **66** (1991) 2720.
- [20] E.G. Drukarev and E.M. Levin, Nucl. Phys. **A 511** (1990) 679.
- [21] M. Lutz, S. Klimt and W. Weise, Nucl. Phys. **A 542** (1992) 521.
- [22] T.D. Cohen, R.J. Furnstahl and D.K. Griegel, Phys. Rev. **C 45** (1992) 1881.
- [23] G.Q. Li and C.M. Ko, Phys. Lett. **B 338** (1994) 118.
- [24] R. Brockmann and W. Weise, Phys. Lett. **B 367** (1996) 40.